journal

J. Am. Ceram. Soc., 90 [1] 16–22 (2007)
DOI: 10.1111/j.1551-2916.2006.01328.x

Macroporous Ceramics from Particle-Stabilized Wet Foams

Urs T. Gonzenbach,† André R. Studart,† Elena Tervoort, and Ludwig J. Gauckler*

Department of Materials, ETH Zürich, Zürich, CH-8093, Switzerland

We present a novel direct-foaming method to produce macroporous ceramics using particles instead of surfactants as stabilizers of the wet foams. This method allows for the fabrication of ultra-stable wet foams that resist coarsening upon drying and sintering. Macroporous ceramics of various chemical compositions with open or closed cells, average cell sizes ranging from 10 to 300 μm and porosities within 45% and 95%, can be easily prepared using this new approach. The sintered foams show high compressive strengths of up to 16 MPa in alumina foams with porosities of 88%.

I. Introduction

Porous ceramics are of great interest due to their numerous potential applications in catalysis, adsorption and separation, filtration of molten metals or hot gases, refractory insulation of furnaces, as well as hard tissue repair and engineering.[1,2] The three main processing routes for the fabrication of macroporous ceramics are the *replica technique*, the *sacrificial template method*, and the *direct-foaming technique*. The processing route ultimately determines the microstructure of the final macroporous ceramic.[3] Therefore, the selection of a given processing method depends strongly on the microstructure needed in the end application, as well as on the inherent features of the process such as cost, simplicity, and versatility.

The direct-foaming technique is particularly suitable for the fabrication of open and closed porous structures with porosities ranging from 45% to 97% and cell sizes between 30 μm and 1 mm.[3] Direct-foaming methods involve the incorporation of a gaseous phase into a ceramic suspension consisting of ceramic powder, solvent, dispersants, surfactants, polymeric binder, and gelling agents. The incorporation of the gaseous phase is carried out either by mechanical frothing, injection of a gas stream, gas-releasing chemical reactions, or solvent evaporation.

The liquid foams obtained upon gas incorporation are thermodynamically unstable due to their large interfacial area. Therefore, gas bubbles that initially nucleated as spheres grow as polyhedral cells. There are mainly three processes responsible for coarsening[4]: drainage and coalescence and Ostwald ripening. Drainage of the liquid from the lamellas between the bubbles results in a close approach of bubble surfaces, which can lead to their coalescence and to foam collapse. Additionally, due to different Laplace pressures of bubbles with different sizes, gas diffusion occurs from smaller to larger bubbles. This migration of gas between bubbles leads to coarsening of the foam and to a broadening of the bubble size distribution. Eventually, the liquid foam collapses due to the combined action of these destabilization mechanisms. Additives are often used to avoid foam collapse by setting the foam structure shortly after air incorporation. This usually occurs by gelling or cross-linking organic compounds added to the suspension liquid medium.[5–11] A drawback of these methods is the fact that they cannot avoid rapid bubble growth before the setting reaction takes place, which leads to large average bubble sizes (30 μm–1 mm) and a wide bubble size distribution.[3]

We have recently shown[12] that ultra-stable wet foams can be produced by using particles instead of surfactants as foam stabilizers in the direct-foaming method. The energy gain upon adsorption of a particle to the air–water interface of fresh gas bubbles can be as high as thousands of kT's, as opposed to the adsorption energy of a few kT's in the case of surfactants (k is the Boltzmann constant and T is the temperature). Therefore, particles can irreversibly adsorb at the surface of gas bubbles, in contrast to surfactants that adsorb and desorb at relatively short time scales at the interface.[13]

The formation of ultra-stable wet foams requires the adsorption of partially hydrophobic particles to the air–water interface. Partial hydrophobization can be achieved through the physical or chemical adsorption of short-chain amphiphilic molecules on the particle surface.[12] The short molecules adsorb with their polar head group onto the particle,[14] leaving the hydrophobic tail in contact with the aqueous solution. Owing to their surface hydrophobicity, particles adsorb onto air–water interfaces and reduce the foam overall free energy by removing part of the highly energetic gas–liquid interfacial area. Foam formation is therefore based on two consecutive assembly processes, namely the adsorption of short-chain amphiphilic molecules on the particle surface and the adsorption of these partially hydrophobized particles onto the air–water interface of freshly incorporated bubbles. Through these assembly processes, a three-level hierarchical structure is formed, containing short-chain amphiphilic molecules in the molecular scale, partially hydrophobized particles in the colloidal scale, and finally air bubbles in the macroscopic scale.[12]

The aim of this work is to investigate the stabilization of foams with colloidal particles and the development of a processing route for the fabrication of solid macroporous ceramics with a tailored microstructure. In order to illustrate the main features of this new process, we used mainly alumina powder and short-chain carboxylic acids as particles and amphiphiles, respectively, for foam stabilization. These molecules show a high solubility in water and are thus suitable for the surface modification of a high concentration of particles in the initial suspension. In this article, the entire processing route to obtain the macroporous ceramics is outlined, and the final microstructure and mechanical properties of the porous structures produced are described.

II. Materials and Methods

(1) Materials

Experiments were carried out using high-purity α-Al_2O_3 powder (HPA-0.5w/MgO, Ceralox, Tucson, AZ) with an average particle diameter (d_{50}) of 200 nm, a specific surface area of 10 m^2/g, and a density of 3.98 g/cm^3. Other chemicals used in the experiments were deionized water, hydrochloric acid (2 N, Titrisol, Merck, Germany), and sodium hydroxide (1 N, Titrisol, Merck). The short-chain carboxylic acids were propionic, butyric, valeric, and enanthic acids (Fluka, Buchs, Switzerland). Table I

G. Franks—contributing editor

Manuscript No. 21696. Received April 12, 2006; approved July 19, 2006.
Supported by CIBA Specialty Chemicals (Switzerland).
*Member, American Ceramic Society.
†Authors to whom correspondence should be addressed. e-mail: urs.gonzenbach@mat.ethz.ch; andre.studart@mat.ethz.ch

Table I. Carboxylic Acids Used to Partially Hydrophobize the Alumina Particles

Compound	Chemical formula	pK_a
Propionic acid	CH_3–CH_2–COOH	4.86
Butyric acid	CH_3–$[CH_2]_2$–COOH	4.83
Valeric acid	CH_3–$[CH_2]_3$–COOH	4.84
Enanthic acid	CH_3–$[CH_2]_5$–COOH	4.89

shows the chemical formulas as well as the pK_a values of these amphiphiles. At a pH equal to the pK_a, 50% of the dissolved molecules are deprotonated. The amphiphile propyl gallate, as well as the gelling agents hydroxyaluminum diacetate ((HADA); $d_{50} \sim 0.7$ μm) and sodium alginate (Fluka AG, Buchs, Switzerland), were later used in this study to produce open-cell macroporous structures.

(2) Suspension Preparation

Suspensions containing carboxylic acids were produced as follows: alumina powder was stepwise added to water containing hydrochloric acid (0.7 wt% to alumina) to obtain a suspension with a solids loading of 50 vol%. Homogenization and deagglomeration were carried out in a ball mill for at least 18 h using polyethylene milling pots and alumina balls (10 mm diameter, ratio balls:powder ~ 2:1). An aqueous solution containing the amphiphile and, if necessary, pH-adjusting agents were then slowly and dropwise added to the ball-milled suspension under slight stirring to avoid local particle agglomeration and coagulation. Afterwards, the pH was set to its desired value and the amount of water needed to achieve certain solids contents was added.

Suspensions containing propyl gallate as an amphiphile were prepared by stepwise adding alumina powder to water containing 506 mmol/L NaOH and 29 mmol/L propyl gallate. The suspension solids loading and pH were initially fixed to 50 vol% and 9.8, respectively. Homogenization of the suspensions was carried out as described above. Afterwards, the propyl gallate needed to adjust the amphiphile concentration in the final suspension to 100 mmol/L was dissolved in a NaOH aqueous solution displaying a pH higher than 10. This solution was then slowly and dropwise added to the ball-milled suspension under slight stirring to avoid local particle agglomeration. Finally, the pH was set to 9.9 and the solids loading to 20 vol% by adding water to the suspension.

(3) Adsorption Measurements

For the adsorption measurements, alumina suspensions were prepared as described above. After ball milling, the carboxylic acid was dropwise added to the suspension, the pH was set to 4.75, and the solids loading to 35 vol% alumina. The suspensions were stirred for 2 h to achieve equilibrium conditions. Two tubes, each filled with 45 mL of suspension, were then centrifuged (Z 513 K, Hermle, Wehingen, Germany) for 1 h at a speed of 4500 rpm. The supernatant obtained was again centrifuged (5417R Eppendorf, Leipzig, Germany) using 16 small tubes, each containing 1.5 mL of the supernatant. In this case, the centrifugation time was set to 20 min and the rotation speed was 15 000 rpm. The pH of the resulting supernatant was set to a value higher than 10 to ensure complete deprotonation of the amphiphilic molecules. The amphiphile concentration in the supernatant was measured by titrating the solution to a pH lower than 2 using either 1 or 0.1 N HNO_3. An automatic titration unit (DT1200, Dispersion Technologies Inc., Mount Cisco, NY) was used for these measurements.

(4) ζ-Potential Analysis

ζ-potential measurements (DT1200, Dispersion Technologies Inc.) were conducted in 2 vol% alumina suspensions at pH 4.75 to assess the effect of the amphiphilic molecules on the surface charge of the alumina particles. For each amphiphile concentration, a new suspension was prepared and ultrasonicated for 5 min before the measurement.

(5) Rheological Tests

The rheological behavior of the suspensions was evaluated using a vane configuration in a stress-controlled rheometer (Model CS-50, Bohlin Instruments, Cirencester, U.K.). The measurements were performed under steady-shear conditions by applying a stepwise stress increase until a shear rate of about 200 s^{-1} was reached. The solids loading of the suspension was 35 vol% alumina at pH 4.75.

(6) Surface Tension Measurements

The surface tension of the suspensions was measured using the pendant drop method (PAT1, Sinterface Technologies, Berlin, Germany). Alumina suspensions were prepared as mentioned above, by dropwise adding the carboxylic acid, setting the pH to 4.75, and diluting the suspension to a solids loading of 35 vol% alumina. Depending on the surface tension of the suspension, the drop volume was set to a constant value within the range 12–35 mm^3.

(7) Foaming and Foam Characterization

Foaming of 150 mL suspensions was carried out using a household mixer (Kenwood, Major Classic, Schumpf AG, Baar, Switzerland) at full power (800 W) for 3 min. The foam density was measured with a custom-built tool, which consisted of a plastic cylindrical cup with small holes on the bottom and a massive sliding stamp on top. The foam was carefully filled into the cup and then slightly compressed with the stamp to remove possible air pockets introduced during filling. The volume between the bottom of the stamp and the bottom of the cylinder was kept constant. Dividing the mass of the foam by its volume resulted in the foam density. The bubble size distribution of the wet foams was evaluated using an optical microscope in transmission mode (Polyvar MET, Reichert-Jung, Austria) connected to a digital camera. The bubble sizes were measured with the linear intercept method using the software Lince (Linear Intercept, TU Darmstadt, Germany).

(8) Foam Setting and Drying

To avoid crack formation during drying, the wet foams were strengthened before water evaporation by either coagulating the particles within the foam lamella or by chemically gelling the foam liquid phase.

In the case of wet foams containing carboxylic acid, the particles within the foam lamella were coagulated by changing the pH *in situ* from 4.75 to 7.5 using the enzyme-catalyzed hydrolysis of urea (Sigma-Aldrich, Buchs, Switzerland).[15] The urea content in the suspensions was 0.05 wt% with respect to alumina and the concentration of the enzyme urease (Roche Diagnostics GmbH, Mannheim, Germany) was 1 U/g alumina. The enzymatic activity of the urease used was 58 000 U/(g of pure urease). One unit is defined as the amount of enzyme necessary to release 1 μmol of reaction product per minute from the substrate at 24°C and at the pH where the enzymatic activity in water is at its maximum. Urea was added to the suspension before homogenization, whereas urease was dissolved in water and added to the suspension before the foaming step.

In the case of wet foams containing propyl gallate as an amphiphile, the foam liquid phase was gelled using the time-delayed gelation between sodium alginate and HADA as described elsewhere in the literature.[16] In order to distribute homogeneously the gelling agent within the suspension, sodium alginate was first dissolved in water at 80°C. After cooling to room temperature, the alginate solution was added to the suspension under stirring. The amount of alginate added corresponded to 0.25 wt% with respect to the mass of alumina in the final suspension. The pH of the suspension was then set to 9.9,

and the amount of water needed to achieve a solids content of 20 vol% was added. In order to slow down the gelation process, the suspension was cooled in ice before foaming. HADA was then added as a powder to the suspension under stirring. The weight ratio HADA:sodium alginate was 7:1. Foaming was finally conducted by mechanical frothing as described.

The resulting wet foams were hand shaped into cylindrical parts (diameter: 100 mm; height: 50 mm) and subsequently dried in air at 22°–25°C for 24–48 h.

(9) Sintering of the Foams

Sintering of the cylindrical dried foams was performed in an electrical furnace (HT 40/16, Nabertherm, Germany) at 1575°C for 2 h. The heating rate was set to 1°C/min and the cooling rate to 3°C/min.

(10) Compressive Strength Measurements

Compressive strength measurements were performed on a universal testing machine (Instron 8562, model A1477-1003, Norwood, MA). A bulk piece of ceramic foam was ground on both sides, resulting in parallel opposite surfaces that ensured homogeneous sample loading during compression. Cylindrical samples with diameters of 15 mm and lengths of 30 mm were drilled out of this bulk piece of foam with a diamond core drill and crushed under a compression speed of 0.5 mm/min.

III. Results and Discussion

(1) Amphiphile Adsorption and ζ Potential

The formation of stable foams requires the adsorption of particles on the surface of freshly incorporated air bubbles.[12] In order to enable their adsorption at the gas–liquid interface, particles with a partially hydrophobized surface are needed. In the case of alumina, hydrophobization can be achieved by modifying the particle surface with short-chain carboxylic acids that adsorb with the carboxylate group onto alumina,[14] leaving the hydrophobic tail in contact with the aqueous solution. The surface properties of the resulting modified particles are mainly determined by the concentration of adsorbed amphiphilic molecules and their tail length.

Figure 1 shows that carboxylic acids with chain lengths of up to six carbons adsorb onto alumina particles under acidic conditions. All measurements were carried out in suspensions containing 35 vol% alumina at pH 4.75 and carboxylic acid concentrations typically required to obtain stable foams.[12] Under such conditions, the dissociated carboxylic acid molecules can adsorb electrostatically as counter-ions onto the oppositely charged alumina surface or through ligand exchange reactions with the alumina hydroxyl surface groups.[14] We observed that the addition of competing counter-ions such as Cl^- to the suspension decreased the amount of adsorbed carboxylate molecules, indicating that the amphiphiles are predominantly adsorbed as counter-ions on the particle surface.

The adsorption of the carboxylic acids on alumina was also influenced by the concentration of particles in the suspension. For a constant ratio of added propionic acid to particle surface area of 1.23 μmol/m^2, we observed a linear increase in the amount of adsorbed amphiphiles from 0.44 to 1.11 μmol/m^2 by increasing the suspension solids content from 5 to 35 vol%, respectively. Based on these adsorption data, we estimate an adsorbed amount of propionic acid of 0.35 μmol/m^2 at a solids content of 2 vol%. This estimated value is in good agreement with the data reported by Hidber *et al.*[14] for this particle concentration (0.31 μmol/m^2). The increase in solids content in the above experiments was also accompanied by an increase in the ionic strength of the liquid media. As a result of the increased ionic strength, higher surface charges are developed on the particle surface[17] and higher concentrations of counter-ions are needed for charge neutralization. Therefore, the enhanced adsorption of amphiphilic counter-ions observed at high solids content might result from the increased surface charge developed on the particles at high particle concentrations.

The surface modification accomplished through the adsorption of carboxylic acid molecules also led to a significant reduction of the particle's ζ potential (potential at the shear plane), as shown in Fig. 2. Surprisingly, this reduction strongly depends on the tail length of the amphiphilic molecule and is far more pronounced than that achieved with equivalent amounts of the 1:1 electrolyte sodium chloride. The addition of high concentrations of carboxylic acids did not invert the ζ potential sign nor changed the alumina isoelectric point, confirming that these molecules adsorb as counter-ions rather than as specific adsorbing species around the particles. Therefore, the electrical potential on the alumina surface remains constant at 45 mV upon addition of amphiphiles or back electrolyte. On the other hand, the ζ potential is strongly influenced by the concentration and valency of counter-ions in the diffuse layer that screen the particle surface charge.[18] The stronger screening effect of amphiphiles as compared with a standard electrolyte (Fig. 2) might result from the specific adsorption of additional anions onto the partially hydrophobized particle surfaces. The hydrophobicity imparted by the first layer of deprotonated amphiphiles adsorbed on the surface leads to an energetically unfavorable exposure of hydrophobic species into the aqueous phase. This favors the adsorption of additional molecules from the aqueous phase onto

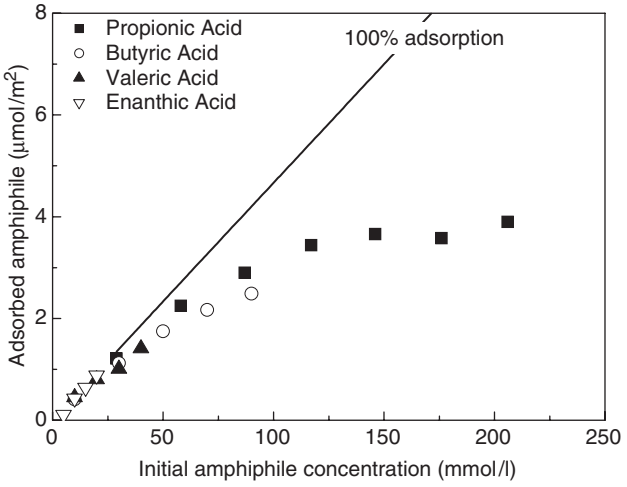

Fig. 1. Adsorption of short-chain carboxylic acids on alumina particles: propionic acid (■), butyric acid (○), valeric acid (▲), and enanthic acid (▽). Measurements were obtained from 35 vol% alumina suspensions at pH 4.75.

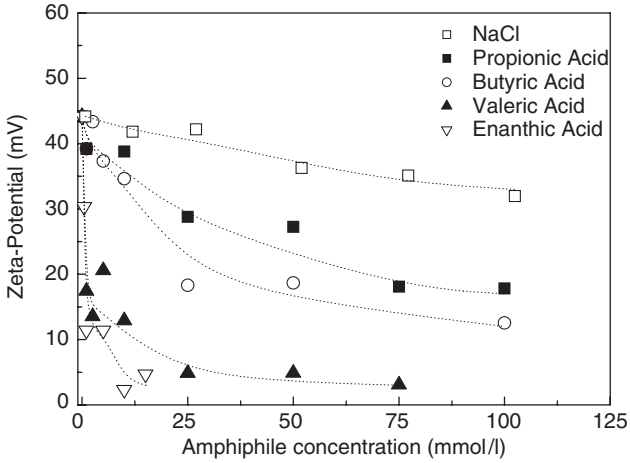

Fig. 2. ζ-potential measurements of 2 vol% alumina suspensions containing NaCl (□), propionic acid (■), butyric acid (○), valeric acid (▲), or enanthic acid (▽).

the particle surface to decrease the system free energy. Hydroxyl ions are known to adsorb specifically on hydrophobic surfaces in contact with water.[19] Likewise, deprotonated amphiphiles might also adsorb as a second layer on the particle surface in a configuration similar to hemi-micelles. In both cases, a negative charge would be added to the particle surface, further screening the positive charges on the particle surface. The effect is more pronounced for amphiphiles with longer hydrophobic tails, as these can lead to an increased surface hydrophobicity at the same concentration in solution (Fig. 2). The hydrophobic interactions between the first layer of adsorbed amphiphiles and the second layer of anions is apparently not strong enough to either invert the particle ζ potential or form a well-defined hemi-micelle around the surface. Most importantly, the second layer of anions does not cover all the hydrophobic surface sites, keeping the particles sufficiently hydrophobic to adsorb at the air–water interface (see Section III (*3*)).

(2) Rheological Behavior

The screening of the particle's surface charge upon amphiphile addition leads to an increase in the suspension viscosity, as shown in Fig. 3. Owing to the surface charge screening, the electrical diffuse layer around the particle surface is not sufficiently thick to overcome the attractive van der Waals forces between particles. This results in particle coagulation and a subsequent increase in the suspension viscosity. Figure 3 shows that the suspension viscosity increases suddenly above a critical concentration of adsorbed carboxylic acid molecules. This critical concentration decreases with an increase in the amphiphile tail length due to the stronger screening effect of the longer molecules (Fig. 2). Besides van der Waals attraction, hydrophobic attractive forces[20–22] might also play a role in the viscosity increase observed in Fig. 3. This hydrophobic attraction is expected to increase upon an increase of the amphiphile tail length.

(3) Surface Tension

The change in particle hydrophobicity upon adsorption of short-chain carboxylic acids can also be monitored by surface tension measurements. The addition of carboxylic acid molecules resulted in a decrease in the surface tension of the suspensions, as illustrated in Fig. 4(a). This decrease is in part due to the free carboxylic acid molecules present in the suspension that adsorb at the air–water interface. The concentration of these free carboxylic acid molecules was determined from the adsorption measurements (Fig. 1), and their contribution to the total surface tension reduction is plotted in Fig. 4(b). The contribution of free amphiphiles was estimated from surface

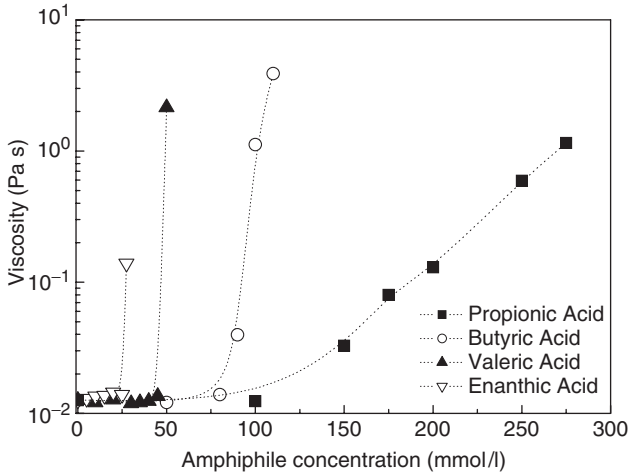

Fig. 3. Viscosity of 35 vol% alumina suspensions at pH 4.75 containing short-chain carboxylic acids with different tail lengths: propionic acid (■), butyric acid (○), valeric acid (▲), and enanthic acid (▽).

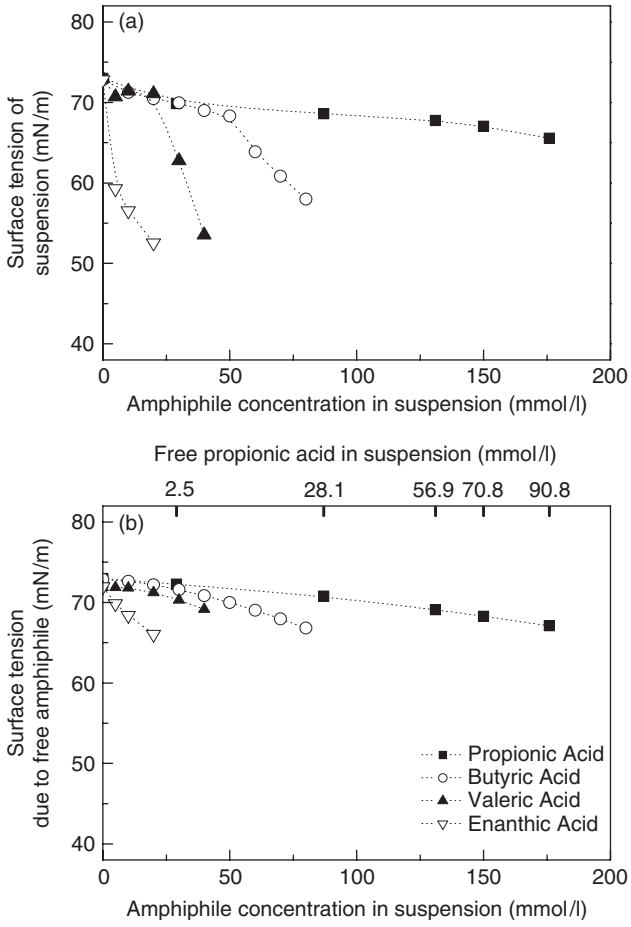

Fig. 4. (a) Surface tension of 35 vol% alumina suspensions at pH 4.75 for different concentrations of carboxylic acids with different tail length (propionic acid (■), butyric acid (○), valeric acid (▲), enanthic acid (▽)). (b) Surface tension of free carboxylic acids in water at pH 4.75. The concentration of free amphiphiles was determined from adsorption measurements of 35 vol% alumina suspensions at pH 4.75 and plotted as top *x*-scale for propionic acid as an example.

tension measurements of aqueous solutions containing carboxylic acid concentrations equivalent to that expected for free amphiphiles in the suspension.

Figure 4(b) shows that the free amphiphiles lead to a gradual and monotonic decrease of the suspension surface tension. On the other hand, Fig. 4(a) indicates that above a certain amphiphile concentration in suspension, the surface tension declines more abruptly than one would expect from the reduction given by the free amphiphilic molecules alone. At this amphiphile concentration, the particles are hydrophobic enough to adsorb to the air–water interface. The adsorbed particles replace part of the highly energetic interface area and lower the overall free energy of the system, leading to an apparent reduction in surface tension of the suspension. The amphiphile concentration needed to render the particles sufficiently hydrophobic to adsorb to the air–water interface decreases markedly with increasing tail length. This can be attributed to the more hydrophobic nature of carboxylic acids with increasing tail length.

(4) Foaming and Foam Stability

The concentration of amphiphilic molecules in the initial suspension and the length of their hydrophobic tail can be used to tailor the degree of surface hydrophobization of the alumina particles in water (see Fig. 4(a)). By providing the proper hydrophobicity on the particle surface, suspensions were homogeneously foamed throughout the whole volume upon mechanical frothing. The mixing speed significantly influences the shear rates and shear stresses applied around the air bubbles during

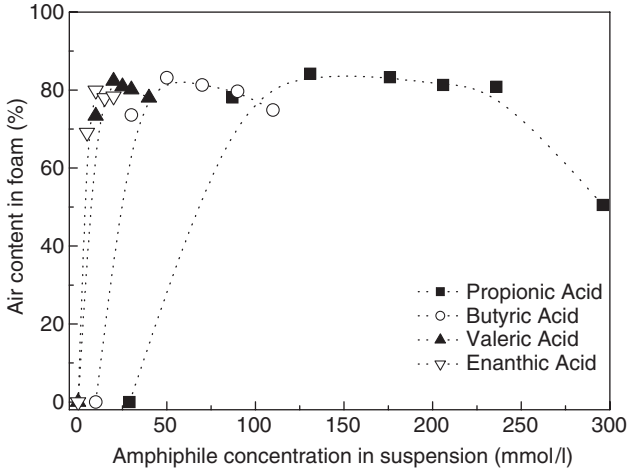

Fig. 5. Air content of foamed suspensions containing 35 vol% alumina at pH 4.75 and different short-chain carboxylic acids: propionic acid (■), butyric acid (○), valeric acid (▲), enanthic acid (▽).

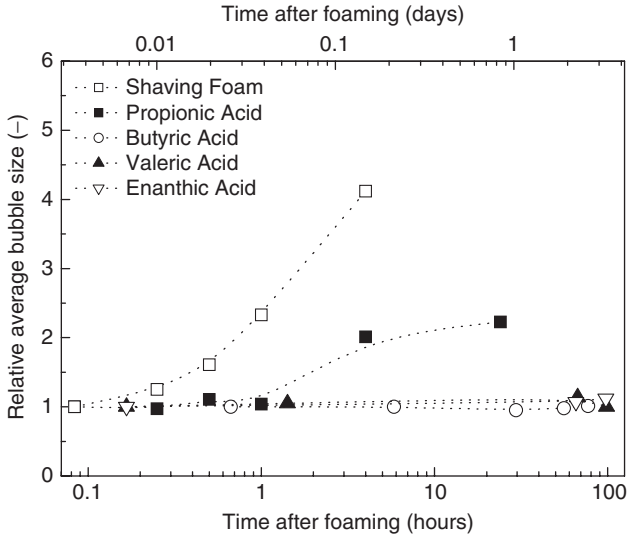

Fig. 6. Relative average bubble size as a function of time after foaming for particle-stabilized foams containing propionic acid (176 mmol/L, ■), butyric acid (50 mmol/L, ○), valeric acid (30 mmol/L, ▲), and enanthic acid (10 mmol/L, ▽) (35 vol% alumina, pH 4.75). The relative average bubble size corresponds to the ratio between actual and initial average bubble size. All data for the particle-stabilized foams were obtained from 35 vol% alumina suspensions at pH 4.75. The stability of a surfactant-stabilized shaving foam (Gillette™) (□) is also included in the graph for comparison.

frothing. Even though the mixing conditions were not investigated here, an increase of the shear stresses applied during frothing should facilitate the mechanical rupture of freshly incorporated bubbles and thus lead to foams with smaller average bubble sizes and narrower bubble size distributions.[23,24]

The wet foams obtained after mixing feature air contents up to 85% (Fig. 5) and possess a high stiffness in the wet state. By increasing the concentration of a given carboxylic acid, the air content of the foam first increases rapidly and then reaches a plateau before decreasing sharply at high amphiphile additions. This sharp decrease at high amphiphile concentrations is attributed to an increase in the viscosity of the initial suspension, caused by the screening effect of counter-ions on the surface charge of the particles (Section III (*2*)). An increased viscosity hinders the incorporation of air into the initial suspension and therefore results in foams with lower air contents.

The as-prepared wet foams exhibit a pronounced yield stress, which allows for shaping of parts using extrusion, injection molding, pressure filtration, or related techniques. The foams can also be sprayed or easily poured into molds after dilution of the as-prepared foams with water. Dilution does not affect the stability of the air bubbles and can be used to adjust the foam viscosity according to the shaping method desired.

The stability of the obtained particle-stabilized foams was compared with that of shaving foam known to be very resistant against destabilization (Gillette Foam, Regular, Gillette Co., London, U.K.). Figure 6 shows that the particle-stabilized foams are stable against bubble growth and drainage over days, whereas the shaving foam shows a rapid bubble growth within the first hours.

The enhanced stability of the foams obtained here is based on the different mechanism used to stabilize the air–water interface compared with that applied in the conventional shaving foam. In the ceramic foams, particles are used as stabilizers, whereas conventional amphiphilic surfactants are used to stabilize the air–water interface in the shaving foam. The energy required to desorb a particle from an air–water interface is orders of magnitude higher than the few kT's needed to desorb a surfactant molecule from the interface.[13] The irreversible adsorption of particles to the interface results in a percolating interfacial armor that mechanically impedes bubble growth, shrinkage, and coalescence.[12] Particles are also expected to form a network throughout the foam lamella, which further prevents bubble coarsening.

(5) Microstructure and Mechanical Strength of Sintered Foams

The high stability of the wet foams allows for drying directly in air at room temperature. However, in order to avoid crack formation during water removal, the wet foam had to be slightly strengthened to overcome the capillary stresses developed during drying and to avoid differential shrinkage within the drying foam. In this work, the strengthening effect was achieved either by coagulating the particles within the foam lamella or by gelling the foam liquid phase. Particles were coagulated *in situ* by shifting the pH from 4.75 to 7.5 using an enzyme-catalyzed decomposition reaction of urea,[15] whereas the gelation of the liquid phase was achieved by cross-linking sodium alginate macromolecules with an ion-releasing agent (see Section II (*8*)).

Figure 7(a) shows the microstructure of a macroporous alumina obtained after drying and sintering a wet foam prepared with butyric acid. In this case, crack formation was avoided by coagulating the particles with the internal pH-shift reaction. The macroporous structure obtained exhibits a total porosity of 88%. Cells are mostly closed with an average size of approximately 35 μm and a standard deviation of 15 μm. Single cells are separated by walls with minimum thicknesses below 1 μm (inset Fig. 7(a)). The foam cells are, in this case, predominantly closed due to the fact that the air bubbles of the original wet foams are completely covered with the surface-modified particles. Such coverage remains through the gelling, drying, and sintering procedure, resulting in the closed cells depicted in Fig. 7(a).

Alternatively, the particle layer that covers the air bubbles of wet foams can also be disrupted during the gelling process to produce macroporous structures with interconnected cells, as shown in Fig. 7(b). Here, the average cell size is in the range of 100–150 μm. In this case, the foam was prepared with propyl gallate and gelled with sodium alginate. The gelation process led to a significant shrinkage of the wet foam. Cell interconnectivity is most likely formed by a local differential shrinkage of the particle layer around the air bubbles during the gelation process. This shrinkage favors the rupture of the particle coating around the bubbles, leading to interconnecting cells after drying and sintering.

The microstructure of our particle-stabilized foams can be tailored to render average cell sizes within the range of 10–300 μm at porosities between 40% and 95%.[3] Compared with surfactant-stabilized foams, our foams can reach smaller average cell sizes and exhibit either open or closed cells even at high

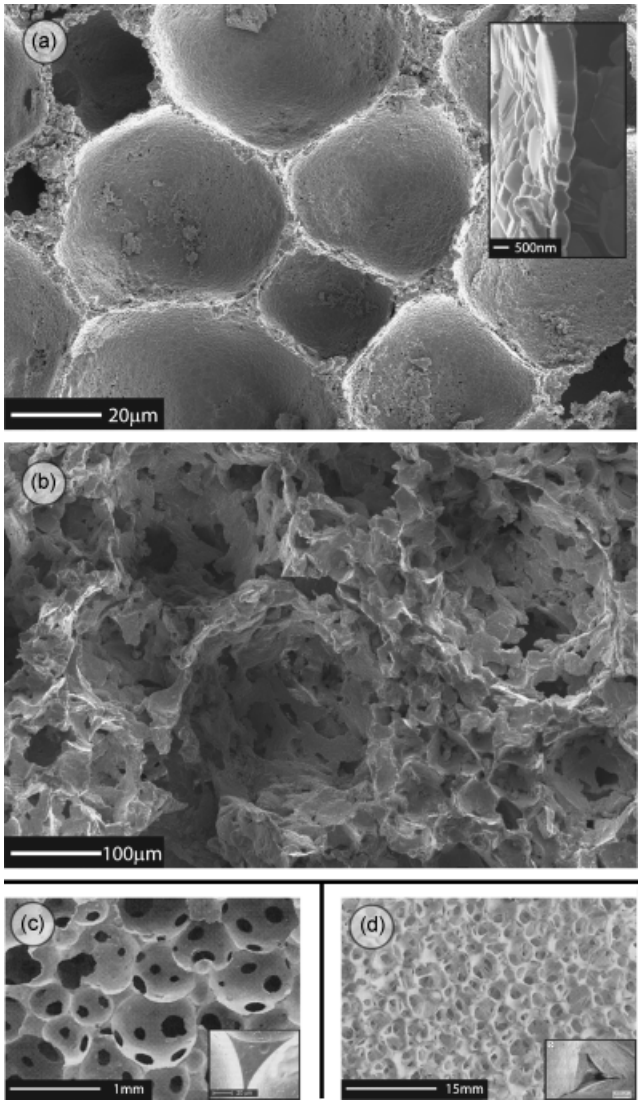

Fig. 7. Microstructures of (a) a close cell particle-stabilized foam, (b) an open-cell particle-stabilized foam, (c) a surfactant-stabilized foam prepared with the direct foaming technique (after Green and Colombo),[25] and (d) a reticulated foam prepared with the replica technique (after Green and Colombo).[25] The insets in (a), (c), and (d) show single struts that are dense in case of the direct foaming technique and hollow in case of the replica technique.

porosities.[3] The smaller cell sizes result from the high stability of the foams in the wet state, which impedes bubble coarsening.

Owing to the possibility to have a closed-cell structure, the maximum compressive strength of our particle-stabilized foams can be higher than that of surfactant-stabilized foams at similar porosities (Fig. 8). In case of surfactant-stabilized foams, the openings between the cells (Fig. 7(c)) are responsible for the lower compressive strength. Such openings arise from the instability of the wet foams before the setting reaction takes place. Foams made by the replica method show an even lower compressive strength due to their highly open-cell structure (Fig. 7(d)) and the presence of cracks and defects in the struts that derive from the burnout of the polymeric material. Additionally, the triangular shape of these defects leads to stress concentrations at the thin edges of the ceramic struts.

The interconnectivity of the cells in case of particle-stabilized foams (Fig. 7(b)) is comparable to that achieved with surfactant-stabilized foams (Fig. 7(c)), but lower than that of foams produced by the replica technique (Fig. 7(d)). However, it is important to note that the preparation of open-cell structures from particle-stabilized foams has not yet been fully exploited and should be thoroughly investigated in future work.

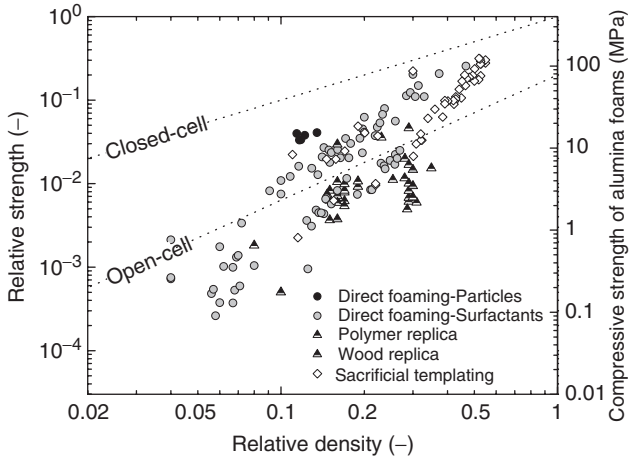

Fig. 8. Compressive strength of our particle-stabilized foams (●, particle network strengthened during drying), compared with foams made by other techniques such as direct foaming with surfactants, replica technique, or sacrificial templating.[3] The relative strength corresponds to the ratio between the strength of the porous and the dense materials. The strength data for the particle-stabilized foams were obtained from samples exhibiting predominantly closed cells.

IV. Conclusions

The *in situ* hydrophobization of colloidal particles in concentrated suspensions allowed for the preparation of high-volume wet foams with air contents up to 85% and bubble sizes between 10 and 300 μm. These foams showed neither bubble growth nor drainage over days. Short-chain carboxylic acids were used to *in situ* hydrophobize the alumina particles used in this work. The degree of particle hydrophobization can be adjusted with the concentration and the tail length of the carboxylic acid molecules added to the suspension. Upon adsorption of these modified particles to the air–water interface, the surface tension of the suspension is significantly lowered. On providing enough hydrophobicity to the particle surface, suspensions were foamed homogeneously throughout the whole volume. Owing to their high stability, these wet foams can be dried in air without bubble coarsening and crack formation. The macroporous ceramics obtained after sintering exhibit porosities of up to 95%, with either open or closed cells between 10 and 300 μm. The mechanical strengths of the sintered foams with closed cells are significantly higher compared with those produced from surfactant-stabilized foams and from polymer replica and sacrificial template techniques. The principles outlined here can also be applied to other ceramic powders, allowing for the preparation of macroporous ceramics with various chemical compositions and tailored final microstructure.

Acknowledgment

The authors would like to thank Philip Sturzenegger, Rahel Nägeli, Claudia Strehler, and Andreas Bihl for their contribution to the experimental work.

References

[1]M. Scheffler and P. Colombo, *Cellular Ceramics: Structure, Manufacturing, Properties and Application*, pp. 645. Wiley-VCH, Weinheim, 2005.
[2]L. L. Hench and J. M. Polak, "Third-Generation Biomedical Materials," *Science*, **295** [5557] 1014–7 (2002).
[3]A. R. Studart, U. T. Gonzenbach, E. Tervoort, and L. J. Gauckler, "Processing Routes to Macroporous Ceramics—A Review," *J. Am. Ceram. Soc.*, **89** [6] 1771–89 (2006).
[4]B. S. Murray and R. Ettelaie, "Foam Stability: Proteins and Nanoparticles," *Curr. Opin. Colloid Interface Sci.*, **9** [5] 314–20 (2004).
[5]P. Sepulveda, "Gelcasting Foams for Porous Ceramics," *Am. Ceram. Soc. Bull.*, **76** [10] 61–5 (1997).
[6]F. S. Ortega, P. Sepulveda, and V. C. Pandolfelli, "Monomer Systems for the Gelcasting of Foams," *J. Eur. Ceram. Soc.*, **22** [9–10] 1395–401 (2002).
[7]F. S. Ortega, F. A. O. Valenzuela, C. H. Scuracchio, and V. C. Pandolfelli, "Alternative Gelling Agents for the Gelcasting of Ceramic Foams," *J. Eur. Ceram. Soc.*, **23** [1] 75–80 (2003).

[8]J. K. Park, J. S. Lee, and S. I. Lee, "Preparation of Porous Cordierite Using Gelcasting Method and its Feasibility as a Filter," *J. Porous Mater.*, **9** [3] 203–10 (2002).
[9]P. Sepulveda and J. G. P. Binner, "Processing of Cellular Ceramics by Foaming and In Situ Polymerisation of Organic Monomers," *J. Eur. Ceram. Soc.*, **19** [12] 2059–66 (1999).
[10]O. Lyckfeldt and J. M. F. Ferreira, "Processing of Porous Ceramics by Starch Consolidation," *J. Eur. Ceram. Soc.*, **18** [2] 131–40 (1998).
[11]A. F. Lemos and J. M. F. Ferreira, *Combining Foaming and Starch Consolidation Methods to Develop Macroporous Hydroxyapatite Implants in Bioceramics*, **Vol. 16**, pp. 1041–4, Trans Tech Publications, Zurich, 2004.
[12]U. T. Gonzenbach, A. R. Studart, E. Tervoort, and L. J. Gauckler, "Ultrastable Particle-Stabilized Foams," *Angew. Chem. Int. Ed.*, **45** [21] 3526–30 (2006).
[13]B. P. Binks, "Particles as Surfactants—Similarities and Differences," *Curr. Opin. Colloid Interface Sci.*, **7** [1–2] 21–41 (2002).
[14]P. C. Hidber, T. J. Graule, and L. J. Gauckler, "Influence of the Dispersant Structure on Properties of Electrostatically Stabilized Aqueous Alumina Suspensions," *J. Eur. Ceram. Soc.*, **17** [2–3] 239–49 (1997).
[15]L. J. Gauckler, T. Graule, and F. Baader, "Ceramic Forming Using Enzyme Catalyzed Reactions," *Mater. Chem. Phys.*, **61** [1] 78–102 (1999).
[16]A. R. Studart, V. C. Pandolfelli, E. Tervoort, and L. J. Gauckler, "Gelling of Alumina Suspensions Using Alginic Acid Salt and Hydroxyaluminum Diacetate," *J. Am. Ceram. Soc.*, **85** [11] 2711–8 (2002).
[17]J. Lyklema, "Fundamentals of Interface and Colloidal Science"; p. 3.21 in *Solid–Liquid Interfaces*, **Vol. II**. Academic Press Inc., San Diego, 1995.
[18]P. C. Hiemenz and R. Rajagopalan, *Principles of Colloid and Surface Chemistry*, 3rd edition, Marcel Dekker Inc., New York, 1997.
[19]J. K. Beattie and A. M. Djerdjev, "The Pristine Oil/Water Interface: Surfactant-Free Hydroxide-Charged Emulsions," *Angew. Chem. Int. Ed.*, **43** [27] 3568–71 (2004).
[20]J. Israelachvili and R. Pashley, "The Hydrophobic Interaction is Long-Range, Decaying Exponentially with Distance," *Nature*, **300** [5890] 341–2 (1982).
[21]H. K. Christenson and P. M. Claesson, "Direct Measurements of the Force Between Hydrophobic Surfaces in Water," *Adv. Colloid Interface Sci.*, **91** [3] 391–436 (2001).
[22]I. Ametov and C. A. Prestidge, "Hydrophobic Interactions in Concentrated Colloidal Suspensions: A Rheological Investigation," *J. Phys. Chem. B*, **108** [32] 12116–22 (2004).
[23]G. I. Taylor, "The Viscosity of a Fluid Containing Small Drops of Another Fluid," *Proc. R. Soc. London Ser. A-Containing Papers Math. Phys. Character*, **138** [834] 41–8 (1932).
[24]C. F. Welch, G. D. Rose, D. Malotky, and S. T. Eckersley, "Rheology of High Internal Phase Emulsions," *Langmuir*, **22** [4] 1544–50 (2006).
[25]D. J. Green and R. Colombo, "Cellular Ceramics: Intriguing Structures, Novel Properties, and Innovative Applications," *MRS Bull.*, **28** [4] 296–300 (2003). □